RSC Advances

PAPER

View Article Online
View Journal | View Issue

Cite this: *RSC Adv.*, 2023, **13**, 11062

Modification of sulfonated poly(arylene ether nitrile) proton exchange membranes by poly(ethylene-*co*-vinyl alcohol)†

Hao Liu,‡[ab] Tiandu Dong,‡[b] Mingzheng Zhou,‡[b] Zetian Zhang,[b] Yunxi Li,[b] Chuanrui Lu,[b] Yichen Liu,[b] Shengqiu Zhao,[a] Shuhong Zheng,[a] Zihan Meng[a] and Haolin Tang *[ab]

The modification of the physicochemical properties of sulfonated poly(arylene ether nitrile) (SPAEN) proton exchange membranes was demonstrated by poly(ethylene-*co*-vinyl alcohol) (EVOH) doping (named SPAEN-*x*%). By controlling the temperature during membrane preparation, the side reactions of the sulfonic acid groups to form sulfonic acid esters were effectively prevented, greatly reducing the proton conductivity of the membranes. Due to the flexible chain of EVOH, SPAEN-8% showed a relatively high elongation of 30.2%, which enhanced the aromatic polymers' flexibility. The SPAEN-2% membrane exhibited proton conductivity of 166, 55, and 9.6 mS cm^{-1} at 95%, 70%, and 50% relative humidity, respectively, higher than those of the other SPAEN-*x*% membranes and even comparable to that of Nafion 212. The water uptake, morphological study, and through-plane proton conductivity of the membranes were studied and discussed. The results suggest that EVOH doping can be used as an effective strategy to improve SPAEN-based proton exchange membranes' performance.

Received 29th December 2022
Accepted 11th March 2023

DOI: 10.1039/d2ra08294b

rsc.li/rsc-advances

Introduction

In recent years, proton exchange membrane fuel cells have been regarded as promising energy conversion devices due to their environmental friendliness and high efficiency. Proton exchange membranes (PEMs), as one of the core components of the fuel cell, are responsible for separating the two electrodes and conducting protons.[1–6] Therefore, numerous polymer materials have been developed to improve the performance of PEMs. The most widely used commercial membranes are based on perfluorosulfonic acid polymers, such as Nafion (Dupont), Aquivion (Solvay), and 3 M polymers, synthesized from tetrafluoroethylene and sulfonyl fluoride vinyl ether.[7,8] Such polymers have high proton conductivity and excellent mechanical properties.[8,9] However, they suffer from harsh reaction conditions and are extremely difficult to recycle.[9]

To overcome these shortcomings, non-fluoroaromatic polymers have been investigated, such as sulfonated poly(arylene ether ketone),[8,10–13] sulfonated poly(arylene ether sulfone),[14–17] sulfonated poly(arylene ether nitrile),[9,18–20] and sulfonated poly(phenylenes).[21–24] However, most non-fluoroaromatic polymers are main-chain-type random copolymers, and they are brittle at low humidity. Their proton conductivity highly depends on the ion exchange capacity (IEC) value.[8,25,26] Thus, organic or inorganic substances have been added to polymer dispersions to improve their physical, chemical, and electrochemical properties.[27] For instance, the Zhang group employed sulfonated graphene oxide to enhance the proton conductivity of the chitosan membrane.[28] The Tan group reported that 3,4-dimethyl benzaldehyde (DMBA) acted as a self-organization assistant that can increase the crystallinity and proton conductivity of membranes.[29] Moreover, the Sun group constructed highly transparent and water-enabled healable antifogging and frost-resisting films based on poly(vinyl alcohol) (PVA)–Nafion complexes.[30] However, these additives displayed poor solubility in the polymer solution, preventing the uniformity of membranes.

In this work, we added different proportions of poly(ethylene-*co*-vinyl alcohol) (EVOH) to the SPAEN solution and cast them onto membranes. The chemical structure of EVOH is shown in Scheme 1. Owing to the high ductility and

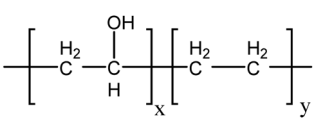

Scheme 1 Chemical structure of EVOH.

[a]State Key Laboratory of Advanced Technology for Materials Synthesis and Processing, Wuhan University of Technology, Wuhan 430070, China. E-mail: thln@wut.edu.cn
[b]State Power Investment Corporation Hydrogen Energy Company, Ltd. Co., Beijing, China

† Electronic supplementary information (ESI) available. See DOI: https://doi.org/10.1039/d2ra08294b

‡ Hao Liu, Tiandu Dong and Mingzheng Zhou contributed equally to this work.

hydrophilicity of EVOH, the mechanical and electrochemical properties of SPAEN-*x*% membranes were greatly improved.[31–33] The key properties of the membranes such as the calculated IEC, water uptake, proton conductivity, tensile strength, Young modulus, elongation, and morphology were studied and discussed in detail.

Experimental

Materials

2,6-Difluorobenzonitrile (DFBN) was purchased from Tokyo Chemical Industry (TCI) and used as received. Potassium 2,5-dihydroxybenzenesulfonate (PDHB) was purchased from Sigma Aldrich and used as received. Hexafluorobisphenol A (6F-BPA) and lead acetate were purchased from Macklin and used as received. Dry dimethyl sulfoxide (DMSO) was purchased from Alfa Aesar and used as received. Poly(ethylene-*co*-vinyl alcohol) (EVOH) was provided by Kuraray Company and purified by the dissolution–precipitation process. Potassium carbonate was used after dehydration.

Synthesis of SPAEN

Typically, to a three-necked flask equipped with a mechanical stirrer, DFBN (3.2 eq., 2.0000 g), PDHB (2.2 eq., 2.4068 g), 6F-BPA (1 eq., 1.4995 g), and dry DMSO (29.5 mL) were added with nitrogen inlet/outlet. After the monomers were completely dissolved in DMSO, K_2CO_3 (4.8 eq., 2.9808 g) was charged. Then, the solution was heated to 170 °C to react for another 9 h. After the viscous mixture was cooled to room temperature, it was poured into dilute hydrochloric acid (1 M) to remove excess K_2CO_3. The yellowish polymers (SPAEN) were collected and purified by filtration with water and isopropanol. They were dried in a vacuum oven at 80 °C for 12 h (yield: 88%).

Preparation and acidification of SPAEN-*x*% PEMs

A typical procedure for SPAEN-5% preparation is as follows. All PEMs were prepared by the solution casting method. Firstly, SPAEN and EVOH (5% mass of SPAEN) were dissolved in DMSO with a concentration of 50 mg mL^{-1} at 50 °C. Secondly, 10 mL solution was taken out and cast onto a clean plane Petri dish (diameter: 9 cm) and dried in an air-circulating oven at 60 °C for 24 h. Consequently, the Petri dish was placed in a vacuum oven at 60 °C for 24 h to remove the residual DMSO. In this work, we used EVOH mass fractions of 0%, 2%, 5%, and 8%. All membranes were acidified in hydrochloric acid (1 M) at 50 °C for 3 days. Finally, the membranes were washed with deionized water until neutralized and then dried. The clean and flat membranes were obtained (Fig. S1†), and the thicknesses of the membranes were *ca.* 70–80 μm.

Characterization

Nuclear magnetic resonance (NMR). NMR spectra were recorded by Bruker AVANCE III (600 MHz, German) using DMSO-d_6 as the solvent to detect the chemical shifts of different hydrogens on the benzene ring and EVOH.

Fourier transform infrared spectroscopy (FT-IR). FT-IR spectra were recorded by Thermo Scientific Nicolet IS20, and the resolution ratio was 4 cm^{-1}. The scanning range was from 4000 to 400 cm^{-1}.

Thermogravimetric analysis (TGA). TGA was recorded by DTA 6300 (Seiko, Japan) under an N_2 atmosphere. The temperature was firstly raised to 100 °C for 30 min to remove water in polymers. Then, the temperature was further raised to 600 °C at a heating rate of 20 °C min^{-1}. Nickel crucibles were used during TGA measurements.

Transmission electron microscopy (TEM). The morphology of the PEMs was investigated by TEM. Firstly, the membrane samples were immersed in 1 M $Pb(Ac)_2$ aqueous solution at 60 °C for 72 h to ensure the exchange from H^+ to Pb^{2+} and dried in a vacuum oven at 80 °C for 24 h. Secondly, the stained and tailored membrane samples were embedded in epoxy resin, sectioned to 50 nm thickness using Lecia-EM-UC6 at a speed of 1 mm s^{-1}, and placed on copper grids. Images were recorded on Quanta 200 using an accelerating voltage of 80 kV.

Water uptake (WU). The water uptakes for different PEMs were obtained by subjecting the membrane samples to constant temperature and humidity in an oven at 80 °C under 40% and 95% relative humidity (RH) for 2 h. Then, the membrane samples were weighed. The WU can be calculated using eqn (1):

$$\mathrm{WU} = \frac{W_1 - W_0}{W_0} \times 100\% \quad (1)$$

where W_0 and W_1 refer to the weights of the dry and wet membranes, respectively.

Theoretical and calculated IEC. The theoretical IEC (mequiv. g^{-1}) was obtained using eqn (2):

$$\mathrm{IEC}_{\mathrm{theo}} = \frac{1000m}{M} \times (1 - x\%) \quad (2)$$

where m refers to the number of sulfonic acid groups per repeating unit, M refers to the molecular weight of the polymer per repeating unit, and x refers to the mass fraction of EVOH in SPAEN.

The calculated IEC was investigated from ^{1}H NMR spectra using eqn (3):

$$\mathrm{IEC}_{\mathrm{cal}} = \left(1 - \frac{k_1}{k_2} \times \frac{11}{3}\right) \times \mathrm{IEC}_{\mathrm{theo}} \quad (3)$$

where k_1 and k_2 refer to the peak areas of hydrogen for SPAEN (6.3–7.8 ppm) and EVOH (1.2–1.5 ppm), as shown in Fig. S2.†

EW and titrated IEC. The equivalent weight (EW, g mol^{-1}) of PEMs was measured by Titrino Plus 848 by acid–base titration. The membrane samples were immersed in a saturated NaCl aqueous solution for 24 h before the experiment. The titrated IEC was calculated from the EW using eqn (4):

$$\mathrm{IEC}_{\mathrm{titr}} = \frac{1000}{\mathrm{EW}} \quad (4)$$

Proton conductivity. Proton conductivity (σ) was determined using electrochemical impedance spectroscopy from 1 Hz to 1 MHz (Hioki IM3533-01). A two-point probe conductivity cell

with two platinum plate electrodes was fabricated. The cell was placed in a thermo-controlled humid chamber at 80 °C for 2 h before the measurement. Proton conductivity was calculated using eqn (5):

$$\sigma = \frac{d}{t_s w_s R} \quad (5)$$

where d is the distance between the two Pt plates, t_s and w_s are the thickness and width of the membrane film, and R is the measured resistance. In this work, the in-plane proton conductivity and the through-plane proton conductivity were both measured.

Tensile testing. The mechanical properties were recorded by Shimadzu AGS-100NX with thin membrane films (length: 5 cm; width: 1 cm) under a stretching rate of 1 mm s^{-1}. The tensile strength, elongation, and Young's modulus values were found. The Young's modulus was calculated using eqn (6):

$$Y = \frac{F}{A} \times \frac{L}{\Delta L} \quad (6)$$

where F/A refers to the tensile stress of the cross-sectional area of the membranes, and $\frac{\Delta L}{L}$ refers to the relative deformation of the membranes under external force.

Results and discussion

Preparation and characterization of copolymers

In this article, the novel prepared PEMs are named as follows: SPAEN-x%, where -x refers to mass fraction of EVOH in polymer SPAEN. In order to verify the physical and electrochemical properties of SPAEN membranes for different addition of EVOH, we chose the addition of 2%, 5%, and 8% as the research targets. Furthermore, commercial membrane Nafion 212 and SPAEN without any doping, named as pure SPAEN, are listed as the targets of comparison.

Fig. 1 shows the synthetic route and characterization of SPAEN polymers. In Fig. 1a, SPAEN was obtained through the polycondensation of DFBP, PDHB, and 6F-BPA in the presence of potassium carbonate. Due to the existence of $-SO_3K$ groups in PDHB, the reactivity of PDHB becomes relatively low. To acquire SPAEN with a high molecular weight, the reaction temperature was set to 170 °C, and the reaction time was set to 24 h. Furthermore, the ^{1}H NMR spectra of SPAEN can provide the degree of polymerization through the calculation of the ratio of the peak area of hydrogen of DFBP and 6F-BPA (Fig. 1b). For EVOH, the chemical shift from 1.0 ppm to 1.5 ppm belongs to $-CH_2$ groups, the chemical shift from 3.4 ppm to 4.0 ppm belongs to –CH groups and the chemical shift from 4.2 ppm to 4.6 ppm belongs to –OH groups (Fig. S2†). After EVOH doping, the positions of sulfonic acid hydrogens changed from 4.1 ppm to 4.4 ppm due to the interaction with –OH groups on EVOH. Fig. 1c shows the FT-IR spectra of EVOH, pure SPAEN, and SPAEN-x%. For SPAEN and SPAEN-x%, the peaks at 2250 cm^{-1} corresponded to –CN symmetric stretching. The broad peaks at 3000–3650 cm^{-1} belongs to the O–H asymmetric stretching, and the peaks at 1142 cm^{-1} are assigned to the C–O asymmetric stretching. Moreover, the peaks at 2850 cm^{-1} and 2900 cm^{-1} were assigned to C–C symmetric stretching and C–C asymmetric stretching, respectively, confirming that SPAEN was doped with EVOH. The ^{1}H NMR and FT-IR spectra confirmed the structure of SPAEN-x%. Additionally, the operating temperature of the dissolution or casting period was no more than 80 °C to prevent side reactions between hydroxyl and sulfonic acid groups at high temperature and low RH, (Fig. 2). Once the sulfonic acid group and the hydroxyl group dehydrate to form an ester bond, the proton conductivity of the

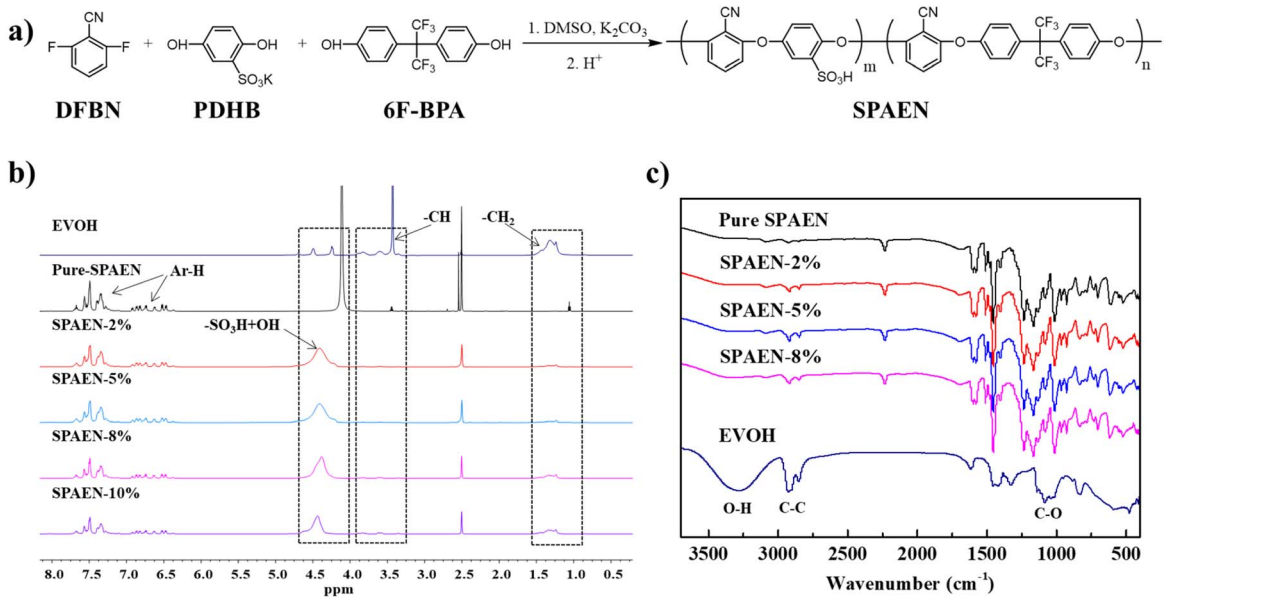

Fig. 1 Synthetic route and characterization of SPAEN polymers. (a) Synthetic route of SPAEN. This random copolymer was prepared from DFBN, PDHB, and 6F-BPA in the presence of potassium carbonate and dry DMSO; (b) ^{1}H NMR spectra of EVOH, pure SPAEN, SPAEN-2%, SPAEN-5%, SPAEN-8%, and SPAEN-10%; (c) FT-IR spectra of EVOH, pure SPAEN, SPAEN-2%, SPAEN-5%, and SPAEN-8%.

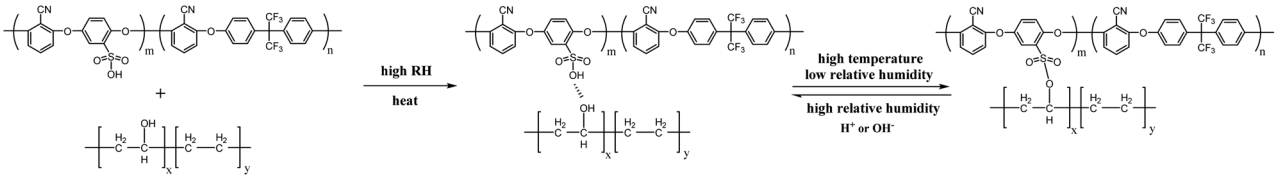

Fig. 2 Interaction between SPAEN and EVOH.

Table 1 Physicochemical properties of SPAEN-*x*% and Nafion 212

		IEC			WU[a]		σ[a]		Mechanical properties[b]		
Code	EW g mol^{-1}	Titr. mequiv. g^{-1}	Theo. mequiv. g^{-1}	Cal. mequiv. g^{-1}	40%	95%	50% mS cm^{-1}	95% mS cm^{-1}	*T* MPa	*E*%	*Y* GPa
SPAEN	420.7	2.38	2.20	2.29	3.8	6.6	11.0	164	70.4	8.8	1.60
SPAEN-2%	455.54	2.20	2.16	2.17	3.8	7.4	9.6	166	79.8	10.6	1.51
SPAEN-5%	461.01	2.17	2.10	2.15	5.8	11.8	8.3	165	72.1	16.8	1.62
SPAEN-8%	471.88	2.12	2.02	2.04	3.5	21.5	6.4	137	81.6	30.2	1.36
Nafion 212	931.87	1.07	—	—	—	—	29.9	142	17.0[c]	320[c]	0.04[c]

[a] 80 °C. [b] 22 °C, 30% RH. [c] Obtained from a previous study.[8]

membranes will be greatly reduced and the polymer will not be soluble in organic solvents. Moreover, the process will not be completely reversible even under strong acid or base. Therefore, the proton conductivity of the SPAEN-*x*% membranes was tested at the RH no less than 50%. Moreover, SPAEN-10% was not selected as the experimental subject because the membrane was opaque after drying.

Physical and chemical properties of SPAEN-*x*% membranes

The physical and chemical properties of pure SPAEN, SPAEN-2%, SPAEN-5%, SPAEN-8%, and Nafion 212 PEMs are listed in Table 1. The EW values of the pure SPAEN and SPAEN-*x*% membranes were 420.7, 455.54, 461.01, and 471.88 g mol^{-1}, respectively. The associated titrated IEC values matched well with the theoretical IEC values, indicating the effectiveness and accuracy of EVOH doping.

Thermal and mechanical properties are the two most significant physical properties of PEMs. Herein, Fig. 3a shows the qualitative estimation of the content of EVOH based on the calculation of the weight loss of the polymer. The –OH groups in EVOH began to degrade at 250 °C and almost completely decomposed at 400 °C. Meanwhile, the thermal properties of the SPAEN-*x*% membranes were greatly affected by EVOH doping. For example, the first weight loss step from 350 °C to 400 °C for the pure SPAEN membrane belonged to the degradation of –SO_3H groups, the polymer main chain further decomposed at above 400 °C. Consequently, the degradation of the blend membranes from 300 °C to 400 °C can be attributed to the sulfonic acid groups and EVOH. Besides, with the increasing of EVOH, ester groups are more likely to form during the heating process, which directly leads to the reduction of hydroxyl groups. The content of hydroxyl groups in SPAEN-5% and SPAEN-8% may not differ much. Thus, the weight of SPAEN-5% and SPAEN-8% showed subtly changed. However, with the temperature rising more than 300 °C, SPAEN-5% and SPAEN-8% will show significantly change only after the ester group is decomposed.

To compare the changes in the mechanical properties of the SPAEN-*x*% PEMs with different EVOH doping percentages, the mechanical properties of pure SPAEN, SPAEN-*x*%, and EVOH

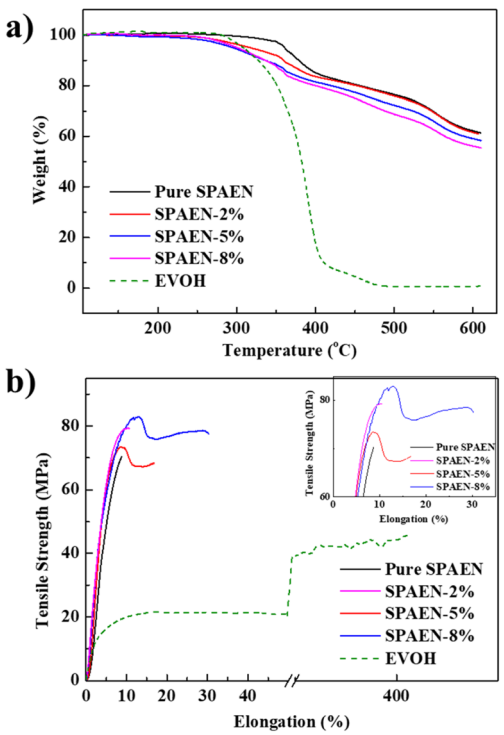

Fig. 3 Physical properties of pure SPAEN, SPAEN-*x*%, and EVOH. (a) TGA curves of pure SPAEN, SPAEN-*x*%, and EVOH; (b) mechanical properties of pure SPAEN, SPAEN-*x*%, and EVOH.

membranes were measured, which can directly affect the preparation of membrane electrode assembly (MEA). Consequently, the PEMs used for MEA were examined in terms of the tensile stress, Young's modulus, and elongation. In Fig. 3b, the elongation of the EVOH membrane reached about 400%, exhibiting great extendibility and flexibility. This superiority is attributed to the block structure of EVOH, that is, the presence of hydrophobic ethylene units and hydrophilic vinyl alcohol units. Moreover, the pure SPAEN membrane showed high tensile stress (70 MPa) and low elongation (8.8%), making it brittle under high temperature and low humidity. After EVOH doping, the SPAEN-*x*% membranes effectively combined the advantages of both EVOH and SPAEN, that is, flexibility and rigidity. With the increase in EVOH, the SPAEN-8% membrane exhibited the highest mechanical properties: a tensile stress of 81.6 MPa, an elongation of 30.2%, and a Young's modulus of 1.36 GPa. Compared with the commercial membrane Nafion 212, the tensile stress of the SPAEN-8% membrane was nearly five times higher than that of Nafion 212 (17.0 MPa). The crosslinking structures tend to make the membranes more rigid, reducing elongation. Therefore, crosslinking side reactions must be avoided.

WU and proton conductivity of SPAEN-*x*% membranes

The WU values of pure SPAEN and SPAEN-*x*% PEMs at 80 °C and 40% and 95% RH are shown in Fig. 4a. It is known that a positive correlation exists between the IEC and the WU. In other words, with the improvement of IEC, the WU of the membranes increases under the same conditions. However, an excessive WU leads to the decline of the volumetric IEC and proton conductivity. Therefore, the control of membrane WU must be investigated. For the pure SPAEN and SPAEN-*x*% membranes at 80 °C and 95% RH, the WU increased with the addition of EVOH, and it became more pronounced as the EVOH content increased. For instance, regardless of a relatively high IEC value of 2.20 mequiv. g^{-1}, the WU of the pure SPAEN membrane was still as small as 6.6% at 95% RH, which can be attributed to the dipole–dipole interactions of nitrile groups. For the SPAEN-8% membrane, although it had a reduced IEC value, the presence of a large amount of hydrophilic EVOH affected dipole–dipole interactions; thus, the WU increased to 21.5%. A similar trend was not reproduced at 40% RH because of the crosslinking side reactions between sulfonic acid and hydroxyl groups at high temperature and low humidity. The dimensional change of SPAEN-*x*% is listed in Table S1.† Even under 95% RH, pure SPAEN and SPAEN-*x*% show no more than 10% change in through-plane or in-plane direction. This phenomenon shows that even if hydrophilic EVOH is doped, the presence of nitrile groups is benefit to inhibit the dimensional change of membranes.

Fig. 4b and c show the in-plane and through-plane proton conductivity of the SPAEN-*x*% membranes under different conditions, together with those of pure SPAEN and Nafion 212 membranes for comparison. The SPAEN-*x*% membranes exhibited low conductivity under low RH conditions. For example, the proton conductivity of the SPAEN-2% membrane exhibited a relatively low proton conductivity of 9.6 mS cm^{-1} under 50% RH, much lower than that of Nafion 212 (29.9 mS cm^{-1}). These results are similar to those of traditional poly(arylene ether) polymers, indicating that polymer EVOH itself is not conductive at low relative humidity. Therefore, the

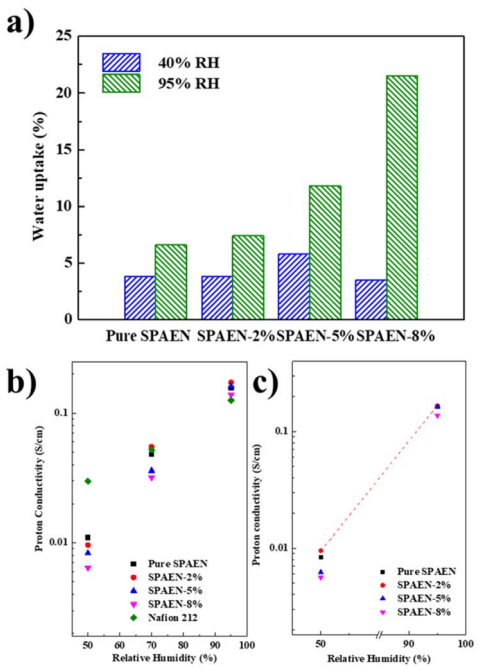

Fig. 4 Water uptake (WU) and proton conductivity of Nafion 212, pure SPAEN, and SPAEN-*x*% membranes at 80 °C. (a) WU of pure SPAEN and SPAEN-*x*% membranes at 40% RH and 95% RH. (b) In-plane proton conductivity of Nafion 212, pure SPAEN, and SPAEN-*x*% membranes at 50%, 70%, and 95% RH. (c) Through-plane proton conductivity of pure SPAEN and SPAEN-*x*% membranes at 50% and 95% RH.

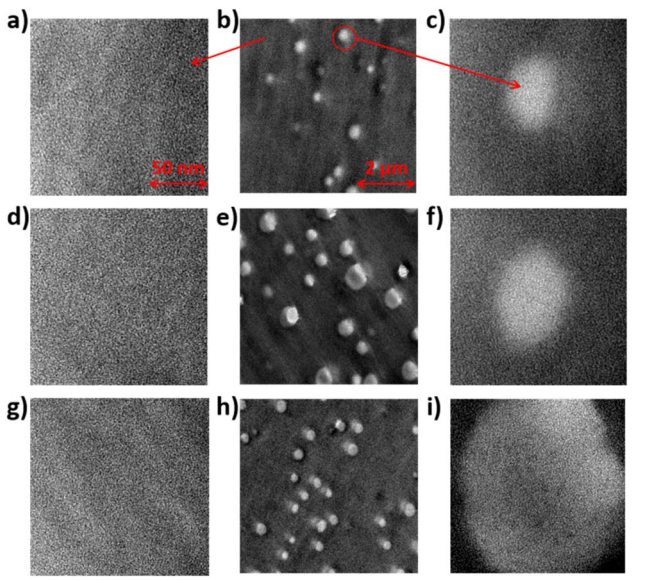

Fig. 5 TEM photographs of SPAEN-*x*% membranes. (a–c) SPAEN-2%, (d–f) SPAEN-5%, and (g–i) SPAEN-8%.

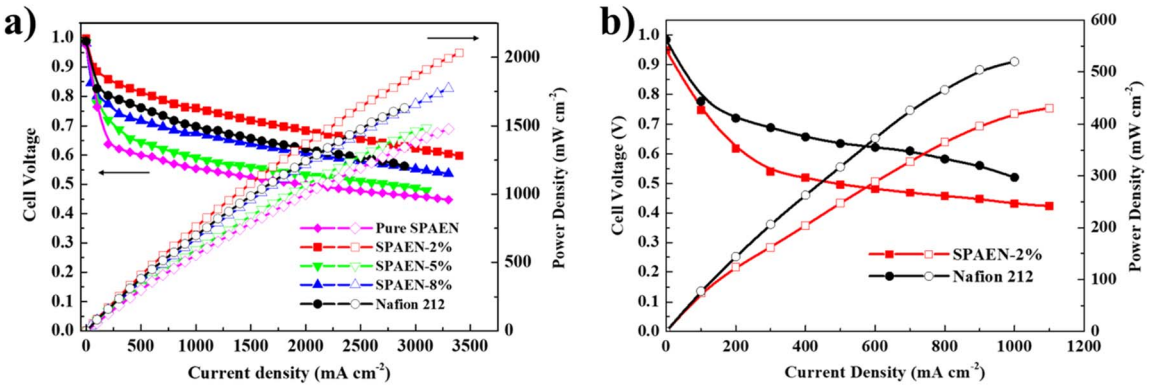

Fig. 6 Fuel cell performance of SPAEN-*x*% and Nafion 212 membranes at 80 °C under (a) 95% RH and (b) 70% RH conditions. The gas feed was fixed at 200 and 500 mL min^{-1} for H_2 and air, respectively.

proton conductivity of the SPAEN-*x*% membranes at low humidity was still dominated by the IEC value. As the RH increased to 70%, the hydrophilicity of EVOH is gradually manifested. The proton conductivity of the SPAEN-2% membrane reached 55 mS cm^{-1} at 70% and 173 mS cm^{-1} at 95% due to its high IEC value and the existence of hydroxyl groups, which can serve as proton exchange pathways. The nano-phase separation of SPAEN-*x*% membranes is presented by TEM and would be discussed in the next chapter.

Morphological analysis of SPAEN-*x*% membranes

Micromorphology plays a significant role in proton conductivity. The morphologies of the pure SPAEN and SPAEN-*x*% PEMs were investigated by TEM analysis. The hydrophilic and hydrophobic regions of pure SPAEN can be discerned in Fig. S3.† In Fig. 5a–i, the dark regions represent the hydrophilic domains, which contain a large amount of Pb^{2+} on sulfonic acid groups, and the bright regions represent the hydrophobic domains, which determine the physical properties. Lead acetate is often used to dye membranes before ultrathin sectioning because of the large atomic number of the lead element. We calculated the domain width to be 4–5 nm, which is in good agreement with the random copolymerization of the polymer system. In Fig. 5b, e and h, EVOHs in the SPAEN-*x*% membranes act as bright spots of similar size (20–30 nm), caused by the low atomic number of alcoholic hydroxyl groups and the difficulty of staining by lead ions. From Fig. 5e–h, the increasing white spots corresponded to the increase in EVOH doping. However, the introduction of EVOH did not change the nano-phase separation. For instance, in Fig. 5a, d and g, the domain widths of the SPAEN-2%, SPAEN-5%, and SPAEN-8% membranes are similar in size (4–5 nm). Additionally, such nano-phase separation could be observed in bright spots in Fig. 5c, f and i, indicating that sulfonic acid groups did not crosslink with hydroxyl groups to form sulfonic acid esters during the membrane formation process and that the change in proton conductivity was caused by the hydrophilicity of EVOH and the WU of the membranes rather than the nano-phase separation.

Oxidative stability and fuel cell performance

The water and oxidation stability of the membranes are listed in Tables S2 and S3,† respectively. In this article, we used Fenton's reagent to simulate the working environment of fuel cells. With the increase of the content of EVOH, the residual weight of the membranes changed from 85.1% to 95.0%, indicating that EVOH could indeed improve the oxidation stability of the membranes. In addition, the weight of SPAEN-*x*% membranes remains stable even in hot water for 36 h. The polarization curves of pure SPAEN, SPAEN-*x*% and Nafion 212 membranes were recorded at 80 °C under 95% and 70% RH in Fig. 6a and b, respectively. For instance, the maximum power density of SPAEN-2% reached about 2000 mW cm^{-2}, which is 20% higher than that of Nafion 212 (about 1600 mW cm^{-2}). By comparison, the maximum power densities of SPAEN-*x*% membranes are determined by their proton conductivities, and the order from high to low is SPAEN-2%, SPAEN-5%, SPAEN-8% and pure SPAEN, respectively. When the humidity drops to 70%, only the power density for SPAEN-2% can be recorded. This phenomenon indicates that although the doping of EVOH helps to improve the fuel cell performance, it is still a huge challenge to improve the performance of non-fluorine materials at low relative humidity.

Conclusions

A series of sulfonated poly(arylene ether nitrile) (SPAEN) with different EVOH doping levels were prepared as PEMs. Pure SPAEN was synthesized using DFBP, PDHB, and 6F-BPA as monomers. A reaction time of 24 h and a reaction temperature of 170 °C were used to ensure SPAEN with a high molecular weight. During the membrane casting period, a temperature less than 60 °C was preserved to prevent dehydration side reactions between hydroxyl and sulfonic acid groups. All as-prepared SPAEN-*x*% membranes showed better malleability than pure SPAEN. The SPAEN-8% membrane exhibited a tensile stress of 81.6 MPa, an elongation of 30.2%, and a Young's modulus of 1.36 GPa. The doping amount of EVOH was largely responsible for the improvement of hydrophilicity and the

introduction of ionic interactions without deteriorating the IEC value, resulting in the higher proton conductivity of the SPAEN-2% membrane at medium-to-high RH. For instance, the proton conductivity of the SPAEN-2% membrane reached 166 and 55 mS cm^{-1} at 95% and 70% RH, respectively, which are comparable to that of Nafion 212 (142 and 47 mS cm^{-1} at 95% and 70% RH). Moreover, all SPAEN-*x*% membranes showed similar phase structures, indicating that the EVOH doping level did not influence the membrane phase structure. Our study demonstrates an effective strategy for the design of high-performance aromatic PEMs under medium to high relative humidity.

Author contributions

Hao Liu, Tiandu Dong and Mingzheng Zhou contributed equally to this work. Hao Liu: conceptualization, methodology, data curation. Tiandu Dong: writing – original draft, conceptualization, methodology, data curation. Mingzheng Zhou: conceptualization, methodology, data curation. Zetian Zhang: methodology. Yunxi Li: methodology. Chuanrui Lu: data curation. Yichen Liu: data curation. Shengqiu Zhao: methodology. Shuhong Zheng: visualization. Zihan Meng: writing – review & editing. Haolin Tang: writing – review & editing.

Conflicts of interest

The authors declare no competing financial interest.

Acknowledgements

This work was supported by the National Natural Science Foundation of China (No. 51976143), the Key Research and Development Program of Guangdong Province (2020B0909040001), and Guangdong Basic and Applied Basic Research Foundation (2020B1515120042).

Notes and references

1 H. Zhang and P. Shen, *Chem. Soc. Rev.*, 2012, **41**, 2382–2394.
2 J. Ran, L. Wu, Y. He, Z. Yang, Y. Wang, C. Jiang, L. Ge, E. Bakangura and T. Xu, *J. Membr. Sci.*, 2017, **522**, 267–291.
3 C. H. Park, C. H. Lee, M. D. Guiver and Y. M. Lee, *Prog. Polym. Sci.*, 2011, **36**, 1443–1498.
4 K. Miyatake, B. Bae and M. Watanabe, *Polym. Chem.*, 2011, **2**, 1919–1929.
5 Z. Shang, R. Wycisk and P. Pintauro, *Energies*, 2021, **14**, 6709–6730.
6 L. Hu, L. Gao, M. Di, X. Yan, X. Jiang, X. Wu, G. He and X. Li, *J. Mater. Chem. A*, 2022, **10**, 3430–3435.
7 R. Devanathan, *Energy Environ. Sci.*, 2008, **1**, 101–119.
8 T. Dong, J. Hu, M. Ueda, Y. Wu, X. Zhang and L. Wang, *J. Mater. Chem. A*, 2016, **4**, 2321–2331.
9 T. Dong, B. He, X. Li, C. Wu, N. Li, M. Ueda, X. Zhang and L. Wang, *J. Polym. Sci., Part A: Polym. Chem.*, 2017, **55**, 1940–1948.
10 J. Pang, X. Jin, Y. Wang, S. Feng, K. Shen and G. Wang, *J. Membr. Sci.*, 2015, **492**, 67–76.
11 D. Qi, C. Zhao, Z. Zhuang, G. Li and H. Na, *Electrochim. Acta*, 2016, **197**, 39–49.
12 Y. Gao, G. P. Robertson, M. D. Guiver, S. D. Mikhailenko, X. Li and S. Kaliaguine, *Macromolecules*, 2004, **37**, 6748–6754.
13 W. Chen, T. Dong, Y. Xiang, Y. Qian, X. Zhao, W. Xin, X. Kong, L. Jiang and L. Wen, *Adv. Mater.*, 2021, 2108410.
14 B. Lafitte, M. Puchner and P. Jannasch, *Macromol. Rapid Commun.*, 2005, **26**, 1464–1468.
15 H. Lee, A. Roy, O. Lane, S. Dunn and J. E. McGrath, *Polymer*, 2008, **49**, 715–723.
16 C. Wang, S. Lee, D. Shin, N. R. Kang, Y. M. Lee and M. D. Guiver, *J. Membr. Sci.*, 2013, **427**, 443–450.
17 Y. Sun, T. Dong, C. Lu, W. Xin, L. Yang, P. Liu, Y. Qian, Y. Zhao, X. Kong, L. Wen and L. Jiang, *Angew. Chem., Int. Ed.*, 2020, **59**, 17423–17428.
18 S. Matsuo, T. Murakami and R. Takasawa, *J. Polym. Sci., Part A: Polym. Chem.*, 1993, **31**, 3439–3446.
19 H. Hu, Y. Sui, M. Ueda, J. Qian, L. Wang and X. Zhang, *J. Membr. Sci.*, 2018, **564**, 342–351.
20 D. W. Shin, S. Y. Lee, C. H. Lee, K. Lee, C. H. Park, J. E. McGrath, M. Zhang, R. B. Moore, M. D. Lingwood, L. A. Madsen, Y. T. Kim, I. Hwang and Y. M. Lee, *Macromolecules*, 2013, **46**, 7797–7804.
21 S. Zhou, Y. Cai, Q. Zhang, J. Zheng, S. Li, Y. Li, S. Zhang and Y. Ding, *J. Membr. Sci.*, 2021, **627**, 119240.
22 T. Mochizuki, M. Uchida and K. Miyatake, *ACS Energy Lett.*, 2016, **1**, 348–352.
23 C. L. Ninivin, A. Balland-Longeau, D. Demattei, C. Coutanceau, C. Lamy and J. M. Léger, *J. Appl. Electrochem.*, 2004, **34**, 1159–1170.
24 F. Liu, J. Ahn, J. Miyake and K. Miyatake, *Polym. Chem.*, 2021, **12**, 6101–6109.
25 S. Lee, J. Ann, H. Lee, J. Kim, C. Kim, T. Yang and B. Bae, *J. Mater. Chem. A*, 2015, **3**, 1833–1836.
26 C. Zhao, H. Lin, K. Shao, X. Li, H. Ni, Z. Wang and H. Na, *J. Power Sources*, 2006, **162**, 1003–1009.
27 M. Feng, Y. Huang, Y. Cheng, J. Liu and X. Liu, *Polymer*, 2008, **144**, 7–17.
28 Y. Liu, J. Wang, H. Zhang, C. Ma, J. Liu, S. Cao and X. Zhang, *J. Power Sources*, 2014, **269**, 898–911.
29 R. Wang, X. Yan, X. Wu, G. He, L. Du, Z. Hu and M. Tan, *J. Polym. Sci., Part B: Polym. Phys.*, 2014, **52**, 1107–1117.
30 Y. Li, X. Fang, Y. Wang, B. Ma and J. Sun, *Chem. Mater.*, 2016, **28**, 6975–6984.
31 Ł. Łancucki and K. Kruczała, *Polym. Degrad. Stab.*, 2014, **109**, 327–335.
32 Y. Zhang, Y. Huang and L. Wang, *Solid State Ionics*, 2006, **177**, 65–71.
33 M. Farrokhi, M. Abdollahi and A. Alizadehb, *Polymer*, 2019, **169**, 215–224.